International Journal of Applied Engineering Research ISSN 0973-4562 Volume 11, Number 15 (2016) pp 8515-8520

Impact of Gaussian Frequency Deviation on the Detection Probability of Power System Harmonics

Diego Bellan
Department of Electronics, Information and Bioengineering, Politecnico di Milano
Piazza Leonardo da Vinci 32, 20133 Milan, Italy
phone: +39-02-23993708; fax: +39-02-23993703; e-mail: diego.bellan@polimi.it

Abstract
This work is devoted to the analytical investigation of the impact of frequency deviation on the detection probability of power system harmonics. In particular, the analysis is performed by assuming a Gaussian distribution of power system frequency around its nominal value. Since additive random noise is always present in actual measurements, detection of low amplitude harmonics can be greatly affected by frequency deviation. Analytical derivations provide explicit expression of the detection probability as a function of the false alarm probability. The role of system parameters, such as signal-to-noise ratio and the standard deviation of the frequency Gaussian distribution, are clearly put into evidence. Analytical results are validated through numerical simulations of the measurement process.

Keywords: Additive noise, Detection probability, Discrete Fourier transform, Harmonic analysis, Power quality, Time-varying frequency.

INTRODUCTION

It is well known that the widespread use of nonlinear and switched components in electrical power systems leads to several power quality issues [1]-[4]. Monitoring of the harmonics content in voltage/current waveforms is one of the most important among such issues. Digital methods for harmonics measurement are well established techniques, mainly based on the evaluation of the discrete Fourier transform (DFT) and further algorithms to improve the accuracy of the measured amplitude, phase and frequency of each harmonic component [5]-[8]. Real time monitoring of a distributed power system, however, prevents the use of sophisticated algorithms because of the heavy computational burden required. Moreover, the need for limiting the computational burden leads to the choice of limiting the number of acquired waveform samples. However, as far as additive noise is concerned, it is well known that a decrease in the number of acquired samples results in higher noise level in the DFT spectra. Therefore, the issue of the detection of low-amplitude harmonics come into play. Such topic was investigated in [9], where the detection probability as a function of the false alarm probability in case of additive noise and use of windows against spectral leakage was addressed. In [9], however, the case of time-varying frequency of sine components was not considered. Frequency fluctuation is an important issue in modern power systems [10], and a thorough power quality analysis cannot disregard this point. As far as harmonic detection is concerned, frequency fluctuation is of paramount importance since it results in a non-coherent sampling of the waveform. As a consequence, the harmonic amplitude is attenuated by the frequency-domain main lobe of the window used against spectral leakage. Thus, frequency instability results in a decreased probability of detection of each harmonic. Therefore, a thorough investigation of harmonic detection probability should include both the effects of additive noise and frequency instability. Such effects are strongly dependent on the specific window used against leakage [11]-[12].

In this paper, the main novelty with respect to [11]-[12] is given by the adopted statistical model for the frequency fluctuation. In fact, a more realistic Gaussian distribution for the harmonic frequencies is considered instead of the simple uniform distribution assumed in [11]-[12].More specifically, the paper is organized as follows. First, previously obtained results are recalled and summarized, concerning in particular the DFT and simplified frequency-domain model of the selected window against spectral leakage. Second, the frequency fluctuation is modeled as a Gaussian random variable, and the corresponding probability density function of the measured spectral line is derived in closed form. Third, the general results concerning detection probability and false alarm probability are recalled, and the specific results obtained through the Gaussian assumption are used to obtain the detection probability including both additive noise and frequency fluctuation effects. Finally, numerical simulations are presented to validate the analytical results derived in the paper.

BACKGROUND AND PROBLEM STATEMENT

Power system harmonics can be measured through digital techniques based on A/D conversion of voltage and current waveforms, and time-to-frequency transformation through the DFT [3], [5]-[12], leading to spectral lines whose amplitude at proper frequency bins represents the magnitude of the measured harmonics.

As far as frequency fluctuation is considered, the fundamental frequency of voltage/current waveforms is typically affected by random instability. It means that by repeating the measurement process, slightly different values of the waveforms fundamental frequency must be expected. Such frequency instability is of course proportionally emphasized for harmonic components. When the DFT is applied, the lack of synchronism between the frequency of the waveform sinusoidal components and the sampling frequency (i.e., non-coherent sampling) will result in increased uncertainty in the amplitude measurements [11]-[12]. Moreover, additive noise

must be included as a source of uncertainty. In fact, voltage/current waveforms are always affected by additive noise which propagates through A/D conversion and DFT transformation, resulting in noisy spectral lines. Of course the frequency-domain impact of additive noise is larger for lower amplitude harmonics. DFT effects of additive noise have been already investigated in many previous papers (e.g., [3], [6], [13]-[16]).

The time-domain voltage waveform is modelled as a sum of *N* harmonically related sine waves and zero-mean white Gaussian noise:

$$v(t) = \sum_{h=1}^{N} V_h \cos(2\pi h f_0 t + \varphi_h) + n(t) \quad (1)$$

A similar expression holds for the current waveform.

After A/D conversion of (1) with sampling frequency f_s, and time window $w(t)$(N_s samples in length) against spectral leakage [5]-[6], the DFT transform provides the estimates of the complex Fourier coefficients:

$$\hat{V}_n = \frac{2}{N_S \mathrm{NPSG}} \sum_{k=0}^{N_S-1} v[k] w[k] \exp(-j2\pi kn/N_S), \quad (2)$$

where NPSG is the Normalized Peak Signal Gain of the selected window (see Tab. 1). The frequency index *n* is related to the frequency index *h* in (1) by $n \times \Delta f = h \times f_0$, where $\Delta f = f_s/N_s$ is the DFT frequency resolution. Under non-coherent sampling, the relation $n \times \Delta f = h \times f_0$ is intended as an approximate relation where *n* is the index such that $n \times \Delta f$ is the discrete frequency closest to $f_h = h \times f_0$.

In the following, the subscripts *n* and *h* will be dropped since the derivations hold for any frequency index.

FREQUENCY FLUCTUATION AS A GAUSSIAN RANDOM VARIABLE

In case of non-coherent sampling condition, the spectral-line magnitude of a harmonic component with frequency f is weighted by the Fourier transform of the time window $w[k]$ used in (2) against spectral leakage. An approximate methodology was introduced in [11]-[12], consisting in the approximation of the frequency-domain behavior of each specific window by a parabolic function obtained by setting the constraint provided by the window Scallop Loss (SL) (see Fig. 1), i.e., the maximum attenuation introduced by the window at the edges $\pm \Delta f/2$ of each DFT bin [5]. From Fig. 1, assuming the *n*-th DFT frequency bin as the origin of the frequency axis, the attenuation introduced by the window on a waveform spectral line can be readily obtained [12]:

Table 1: Some figures of merit of three common windows.

Window	NPSG	ENBW	SL [dB]	SL
Rect.	1	1	3.92	0.637
Hann	0.50	1.50	1.42	0.849
Blackman-Harris min. 4 term	0.36	2	0.83	0.909

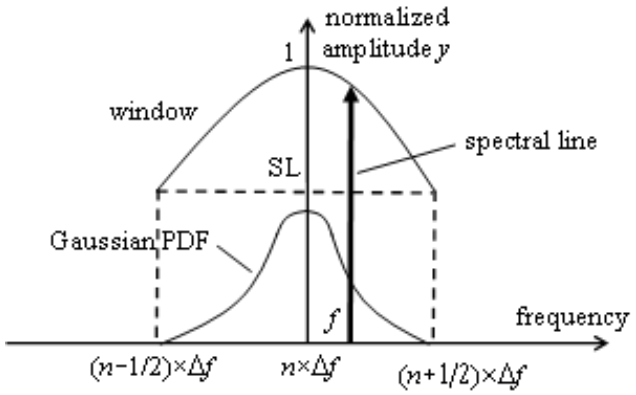

Figure 1: Spectral line with Gaussian frequency distribution and magnitude weighted by the frequency-domain window.

$$y \cong 1 - \frac{4(1-SL)}{\Delta f^2} f^2 \quad (3)$$

Such attenuation is applied to the actual amplitude *V* of each sinusoidal component in (1). Therefore, the measured amplitude of each sinusoidal component can be written:

$$M = yV \quad (4)$$

where *V* denotes the non-weighted frequency-centered spectral line.

In this paper the frequency f is modeled as a zero-mean Gaussian random variable (RV) centered on the DFT frequency bin $n \times \Delta f$ and with standard deviation σ_f such that the distribution can be neglected outside the frequency bin Δf, i.e., $\sigma_f < \Delta f/4$(see Fig. 1). The probability density function (PDF) of *y* can be readily evaluated by resorting to the theorem on the transformation of RV [17]-[19]. Indeed, for a given *y*, from (3) the corresponding frequency (positive root) can be readily obtained:

$$\bar{f} = \frac{\Delta f}{2} \sqrt{\frac{1-y}{1-SL}} \quad (5)$$

The theorem on transformation of RV requires the evaluation of the magnitude of the first derivative of (3) at the frequency in (5):

$$\left| y'(\bar{f}) \right| = \frac{4}{\Delta f} \sqrt{(1-y)(1-SL)} \quad (6)$$

Notice that by considering the negative root of (3) (i.e., (5) with negative sign), the same result (6) would be obtained. Therefore, from the theorem on transformation of RV we obtain that the PDF of *y* is given by two times the PDF of f (i.e., the Gaussian PDF) evaluated in (5) and divided by (6):

$$f_y(y) = \frac{1}{2(\sigma_f/\Delta f)\sqrt{2\pi(1-y)(1-SL)}} \exp\left(-\frac{(1-y)/(1-SL)}{8(\sigma_f/\Delta f)^2} \right) \quad (7)$$

Finally, by taking into account (4), the PDF of the measured harmonic amplitude is given by [17]:

$$f_M(M) = \frac{1}{V}\frac{1}{2(\sigma_f/\Delta f)\sqrt{2\pi(1-M/V)(1-SL)}}\exp\left(-\frac{(1-M/V)/(1-SL)}{8(\sigma_f/\Delta f)^2}\right) \quad (8)$$

DETECTION PROBABILITY AS A FUNCTION OF ADDITIVE NOISE AND FREQUENCY FLUCTUATION

Additive noise $n(t)$ in (1) results in a random behavior of the DFT coefficients $\hat{V}_n$ in (2). The real and the imaginary parts of each $\hat{V}_n$ can be approximated as a Gaussian RV with unbiased mean value (i.e., the deterministic noise-free values), and variance [3], [6]

$$\sigma^2 = ENBW\frac{2}{N_S}\sigma_n^2 \quad (9)$$

where ENBW is the equivalent noise bandwidth of the selected window $w(t)$, and σ_n^2 is the variance of the input noise $n(t)$.

By defining a threshold level α, the false alarm probability is defined as the probability that an only-noise spectral line is larger than α. In [12] it was shown that the false alarm probability is given by

$$P_{fa}(\alpha) = \exp\left(-\frac{\alpha^2}{2\sigma^2}\right) \quad (10)$$

The detection probability is defined as the probability that a signal spectral line is greater than the threshold. In [12] it was shown that the detection probability is given by

$$P_d(\alpha) = Q_1\left(\frac{M}{\sigma}, \frac{\alpha}{\sigma}\right) \quad (11)$$

where Q_1 is the Marcum Q function [20].By solving (10) with respect to α and substituting into (11) we obtain [12]

$$P_d(P_{fa}) = Q_1\left(\frac{M}{\sigma}, \sqrt{-2\log(P_{fa})}\right) \quad (12)$$

Therefore, for a given signal-to-noise ratio M/σ, eq. (12) provides the detection probability as a function of the accepted false alarm probability.

The measured amplitude of a harmonic spectral line is affected by both additive noise and frequency fluctuation. Therefore, the detection probability for a given threshold level α must be obtained from the total probability theorem by combining (11) (representing only the noise contribution for a given harmonic amplitude M) and (8) (representing the frequency fluctuation contribution) [17]:

$$P_d(\alpha) = \int_{SL\cdot V}^{V} P_d(\alpha|M) f_M(M) dM = \int_{SL\cdot V}^{V} Q_1\left(\frac{M}{\sigma}, \frac{\alpha}{\sigma}\right) f_M(M) dM \quad (13)$$

and by taking into account (4) we obtain:

$$P_d(\alpha) = \int_{SL}^{1} Q_1\left(SNR\cdot y, \frac{\alpha}{\sigma}\right) f_y(y) dy \quad (14)$$

where

$$SNR = \frac{V}{\sigma} \quad (15)$$

is the harmonic signal-to-noise ratio.

Finally, by taking into account (12), the detection probability can be expressed as a function of the false alarm probability as

$$P_d(P_{fa}) = \int_{SL}^{1} Q_1\left(SNR\cdot y, \sqrt{-2\log(P_{fa})}\right) f_y(y) dy \quad (16)$$

where $f_y(y)$ is given by (7).

NUMERICAL VALIDATION

Numerical validation of the analytical result (16) was performed by simulating the whole measurement process. According to (1), a voltage waveform consisting of three harmonic components was selected such that $f_0 = 50$ Hz, and $h = 1, 3, 5$. The harmonic amplitudes were selected as $V_1 = 10, V_3 = 2, V_5 = 1$. Phase angles were selected at random. Sampling was performed such that 10 periods of the fundamental component were acquired, i.e., a 200 ms measurement window were taken. The selection of the number of samples N_s defines the corresponding sampling frequency. By assuming $N_s = 2^{12}$ the corresponding sampling frequency was $f_s = 20.48$ kHz, and the related frequency resolution was $\Delta f = 5$ Hz. A repeated run analysis (10^4 runs to estimate each average value) was performed by assuming f_0 taking random values with Gaussian distribution centered on the nominal frequency 50 Hz. Notice that the standard deviation of the fundamental frequency is multiplied by the harmonic order when a harmonic component is considered. In the following, analytical results were validated for the fifth harmonic. Therefore, by denoting as σ_f the standard deviation of the fifth harmonic, the corresponding standard deviation of the fundamental is $\sigma_f/5$. Two different windows against spectral leakage were used, i.e., the rectangular and the minimum 4-term Blackman-Harris windows (see Tab. 1), corresponding to substantially different values of the parameters ENBW and SL. Figure 2 shows the detection probability of the fifth harmonic as a function of the accepted false alarm probability, for the two windows mentioned above. Dashed lines correspond to numerical simulations, whereas solid lines correspond to the analytical result (16). The signal-to-noise ratio (15) was equal to 5, and the standard deviation of the harmonic frequency $\sigma_f = 1$ Hz. Agreement between numerical and analytical results is good. Blackman-Harris window provides a higher detection probability than the rectangular window. Figure 3 differs from Figure 2 in the standard deviation of frequency, i.e., $\sigma_f = 1.25$Hz. Comparison between the two figures shows that by increasing the frequency fluctuation the difference between the detection probability of the two windows increases. This result can be explained by considering that the two windows have very different behavior near the frequency bin edges.

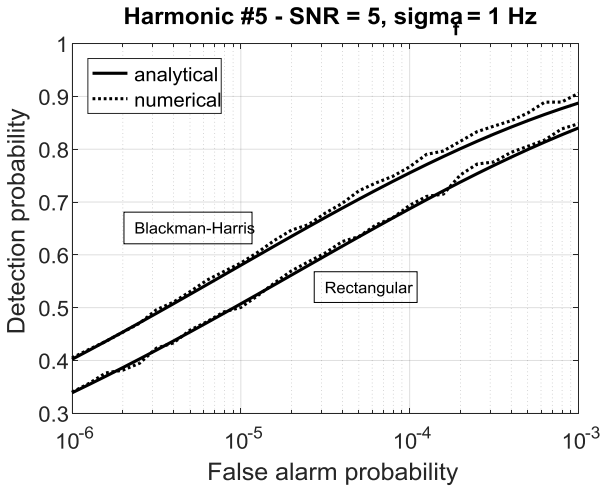

Figure 2: Detection probability of the fifth harmonic as a function of the false alarm probability. Signal-to-noise ratio is 5, and standard deviation of frequency is 1 Hz. Two windows are compared, i.e., rectangular and minimum 4-term Blackman-Harris windows.

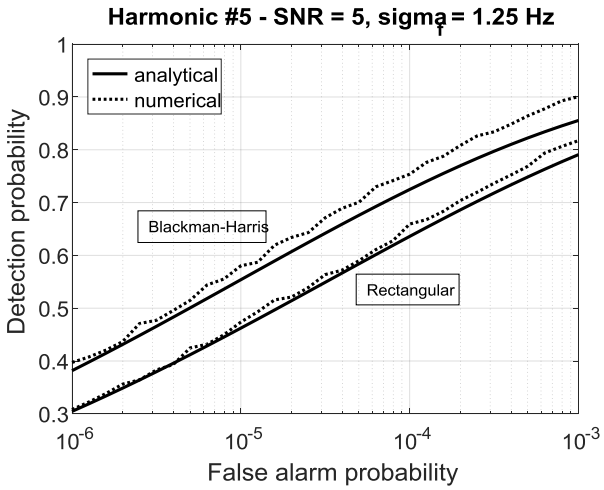

Figure 3: Same as Figure 2, but with standard deviation of frequency equal to 1.25 Hz instead of 1 Hz.

Figures 4 and 5 are similar to 2 and 3, apart from a lower value of signal-to-noise ratio equal to 4. The weight of noise is larger in this case, and therefore the different behavior of the two windows is less apparent, i.e., the curves corresponding to the two windows are closer each other with respect to Figures 2 and 3. Moreover, detection probabilities are lower than in Figures 2 and 3 because of higher noise level.

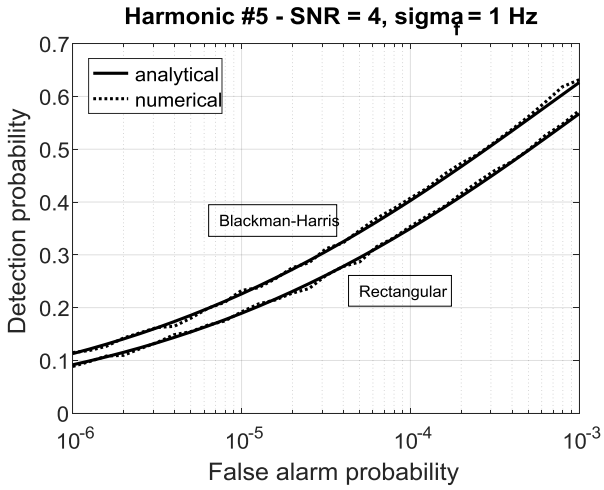

Figure 4: Detection probability of the fifth harmonic as a function of the false alarm probability. Signal-to-noise ratio is 4, and standard deviation of frequency is 1 Hz. Two windows are compared, i.e., rectangular and minimum 4-term Blackman-Harris windows.

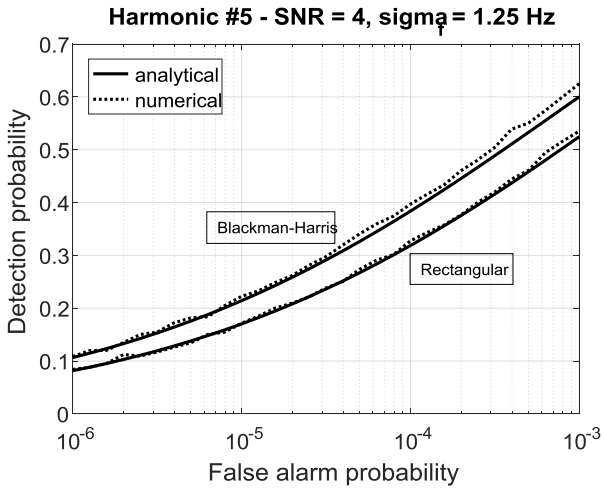

Figure 5: Same as Figure 4, but with standard deviation of frequency equal to 1.25 Hz instead of 1 Hz.

Finally, Figures 6 and 7 are related to even lower value of signal-to-noise ratio equal to 3. The difference between the two windows is even less apparent. In fact, in this case the deterministic behavior of the two windows, i.e., the different frequency-domain main lobe, is masked by the high level input noise.

CONCLUSION

Detection probability of power system harmonics affected by frequency fluctuation with Gaussian distribution has been investigated for different windows and different additive noise levels. It was shown that the frequency-domain shape of the main lobe of the selected window plays a crucial role as the noise level decreases. On the contrary, as the noise level increases, the considered windows provide a similar behavior

with respect to detection capability, especially when a low false alarm probability is required.

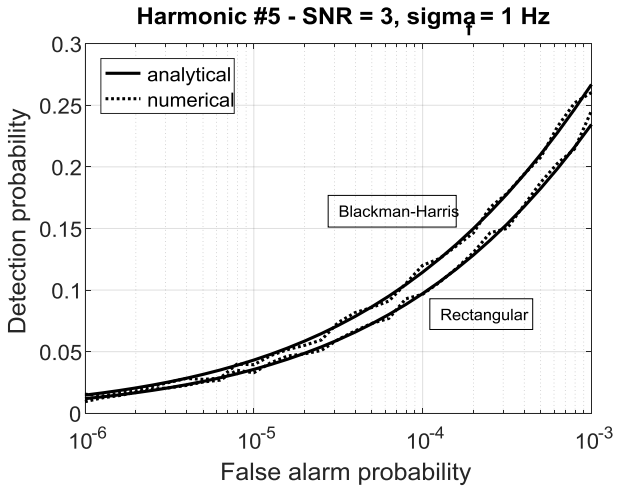

Figure 6: Detection probability of the fifth harmonic as a function of the false alarm probability. Signal-to-noise ratio is 3, and standard deviation of frequency is 1 Hz.

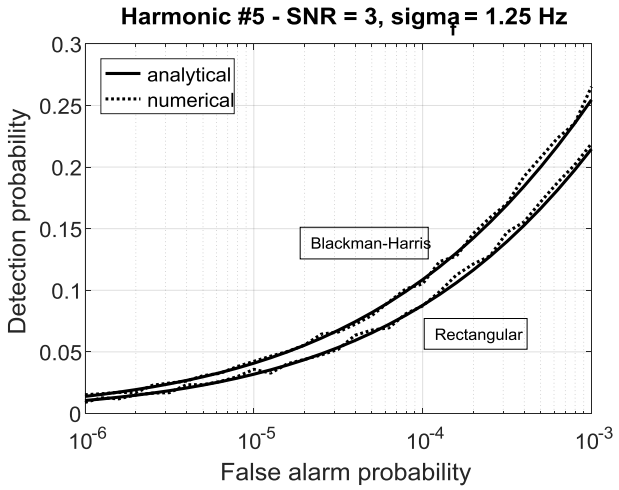

Figure 7: Same as Figure 6, but with standard deviation of frequency equal to 1.25 Hz instead of 1 Hz.

REFERENCES

[1] IEC 61000-4-7, *Electromagnetic compatibility (EMC) – Part 4-7: Testing and measurement techniques – General guide on harmonics and interharmonics measurements and instrumentation, for power supply systems and equipment connected thereto.* IEC, 2002.

[2] D. Bellan, G, Spadacini, E. Fedeli, and S. A. Pignari, "Space-frequency analysis and experimental measurement of magnetic field emissions radiated by high-speed railway systems," *IEEE Trans. Electromagn. Compat.*, vol. 55, no. 6, pp. 1031-1042, 2013.

[3] D. Bellan, "Statistical Characterization of Harmonic Emissions in Power Supply Systems," *International Review of Electrical Engineering*, vol. 9, no. 4, pp. 803-810, 2014.

[4] D. Bellan, G. Superti Furga, and S. A. Pignari, "Circuit representation of load and line asymmetries in three-phase power systems," *International Journal of Circuits, Systems and Signal Processing*, vol. 9, pp. 75-80, 2015.

[5] F. J. Harris, "On the use of windows for harmonic analysis with the discrete Fourier transform," *Proc. of the IEEE*, vol. 66, pp. 51-83, 1978.

[6] O. M. Solomon, "The use of DFT windows in signal-to-noise ratio and harmonic distortion computations," *IEEE Trans. Instrum. Meas., vol. 43*, pp. 194-199, April 1994.

[7] D. Belega, D. Dallet, and D. Petri, "Accuracy of Sine Wave Frequency Estimation by Multipoint Interpolated DFT Approach," *IEEE Trans. on Instrum. Meas.*, vol. 59, no. 11, pp. 2808-2815, 2010.

[8] C. Chen and Y. Chen, "Comparative Study of Harmonic and Interharmonic Estimation Methods for Stationary and Time-Varying Signals,"*IEEE Trans. on Industrial Electronics, vol. 61*, no. 1, pp. 397-404, Jan. 2014.

[9] H.C. So, Y.T. Chan, Q. Ma, and P.C. Ching, "Comparison of various periodograms for sinusoid detection and frequency estimation," *IEEE Trans. Aerospace and Electronic Systems, vol. 35*, pp. 945-952, July 1999.

[10] P. D. Poljak, M. D. Kusljevic, and J. J. Tomic, "Power Components Estimation According to IEEE Standard 1459–2010 Under Wide-Range Frequency Deviations," *IEEE Trans. Instrum. Meas.*, vol. 61, pp. 636-644, Feb. 2012.

[11] D. Bellan, "Frequency Instability and Additive Noise Effects on Digital Power Measurements Under Non-Sinusoidal Conditions, "in *Proc. 2014 6th IEEE Power India International Conference (PIICON)*, Delhi, India, Dec. 5-7, 2014, pp. 1-5.

[12] D. Bellan, "Detection probability of harmonics in power systems affected by frequency fluctuation," *International Journal of Circuits, Systems and Signal Processing*, vol. 10, pp. 254-259, 2016.

[13] D. Bellan, "Characteristic Function of Fundamental and Harmonic Active Power in Digital Measurements Under Nonsinusoidal Conditions," *International Review of Electrical Engineering*, vol. 10, no. 4, pp. 520-527, 2015.

[14] D. Bellan, A. Gaggelli, and S. A. Pignari, "Noise Effects in Time-Domain Systems Involving Three-Axial Field Probes for the Measurement of Nonstationary Radiated Emissions," *IEEE Trans. on Electromagn. Compat.*, vol. 51, no. 2, pp. 192-203, 2009.

[15] D. Bellan, "Noise Propagation in Multiple-Input ADC-Based Measurement Systems,"*Measurement Science Review*, vol. 14, no. 6, pp. 302-307, 2014.

[16] D. Bellan, "On the Validity of the Noise Model of Quantization for the Frequency-Domain Amplitude

Estimation of Low-Level Sine Waves,"*Metrology and Measurement Systems*, vol. 22, no. 1, pp. 89-100, 2015.

[17] A. Papoulis and S. U. Pillai, *Probability, Random Variables and Stochastic Processes*. McGraw-Hill, 4th Ed., 2002.

[18] D. Bellan and S.A. Pignari, "Statistical superposition of crosstalk effects in cable bundles,"*China Communications, vol. 10*, no. 11, pp. 119-128, 2013.

[19] D. Bellan and S. A. Pignari, "Efficient estimation of crosstalk statistics in random wire bundles with lacing cords," *IEEE Trans. on Electromagn. Compat.*, vol. 53, pp. 209-218, Feb. 2011.

[20] M. K. Simon, *Probability Distributions Involving Gaussian Random Variables*. Springer, 2002.